
Proceedings Paper:
Moore, J. orcid.org/0000-0002-5182-9439, Burkinshaw, C. and Sawyer, D. (2025) Machine learning for robotic accuracy improvement in drilling operations. In: IEEE International Conference on Automation Science and Engineering (CASE). 2025 IEEE 21st International Conference on Automation Science and Engineering, 17-21 Aug 2025, Los Angeles, USA. Institute of Electrical and Electronics Engineers (IEEE), pp. 2960-2966. ISBN: 9798331522476. ISSN: 2161-8070. EISSN: 2161-8089.

https://doi.org/10.1109/CASE58245.2025.11163955

Machine learning for robotic accuracy improvement in drilling operations*

James Moore, Chris Burkinshaw, & Daniela Sawyer.

Abstract— **Drilling of rivet/fastener holes in aircraft presents a major manufacturing challenge where manual processes are heavily relied upon. It is estimated that modern aircraft can require upwards of 1.5 million holes to be drilled using methods that involve some form of manual input. This introduces concerns over both hole accuracy and worker wellbeing. Industrial robotic arms offer a potentially promising solution due to their reach and flexibility. However, limitations in their positional accuracy can be a barrier.**

This paper presents an open-loop methodology to address these limitations by improving the positional accuracy of a robotic drilling platform using Gaussian process regression (GPR) models, without the need for permanently installing costly metrology equipment, such as laser trackers or secondary encoders. The models demonstrated an average reduction in the positioning error of the platform from 0.993 mm down to 0.022 mm (97.7%) in x, and from 0.209 mm down to 0.055 mm (73.5%) in y in free air.

This methodology is then demonstrated on physical drilling trials, where the average hole position error was reduced from 0.688 mm to 0.323mm (53.0%) in x. However, due to limitations in the training of the models, the error in y increased from 0.261 mm to 0.378 (45.1%). Despite these results being less successful, it is intended that they serve as a baseline for future development of the methodology so that it can include the effects of process (drilling) forces.

I. Introduction

Despite the trend for automating manufacturing processes over the past few decades, there are still significant gaps in industry where manual processes are heavily relied upon. In particular, the drilling of aircraft components to produce rivet/fastener holes still presents a major challenge, where it is estimated that around 65% of holes are drilled using manual or semi-automated[1] drilling operations [1]. Considering that a typical aircraft can require upwards of 3 million drilled holes, [2] this necessitates a huge amount of manual input. This presents not only the typical quality concerns that arise from manual intervention (i.e. human error); but also concerns over worker wellbeing due to the labour-intensive nature of the operations, as hole locations can be awkwardly positioned (particularly those that are drilled upwards), and automated drilling units can be heavy and cumbersome.

Although introducing robotics seems like an obvious solution due to their flexibility and reach over traditional machining platforms, the positional tolerances for such holes stipulated by *"EN3201:2008 Aerospace series — Holes for metric threaded fasteners"* can be as low as 0.15 mm [3]. This is well below the positional accuracy that can be achieved by off-the-shelf industrial robot arms, which are typically limited to accuracies around 1 mm. The positional errors present in robotic drilling operations can be broken down into three main categories: **robot positional errors**, arising from factors such as build quality issues and low stiffness of serial kinematics [4]; **process (drilling) errors** , which can be a result of issues such as the tool slipping across the surface of the workpiece away from the nominal position [5]; and **workpiece errors**, which could be related to poor geometrical quality of supplied material, or even damage caused during prior operations.

Ideally, it would be possible to utilise in-process measurements of a robot's position to provide closed-loop feedback to correct for any errors due to robot positional error or process error in real-time. This methodology has been demonstrated to be effective using various technologies, with examples from Stadelmann et al. [6] who utilised a combination of iGPS and an inertial measurement unit to improve the mean static end effector position error to 0.10 mm; and from Gharaaty et al. [7] who were successful in using a photogrammetry system to minimise the pose accuracy of a robot to a target of less than 0.050 mm. However, in earlier work conducted at the University of Sheffield Advanced Manufacturing Research Centre (AMRC), Cho et al. [8] concluded that although the addition of permanent external measurement technology (vision or laser-based systems) has been shown to provide accuracy improvements, the additional cost and complexity that such systems introduce may be prohibitive. Instead, it is suggested that implicit methods (i.e. using data already available from the robot's controller alongside a corrective model) might be a more viable option for industry.

The long-term aim of this work is to create a combined model that can correct for both robot positional errors and process errors. However, the initial piece of work presented in this paper focuses on correcting only the robot positional error. This has the advantage of developing a methodology that is not only suitable for drilling operations but that could be adapted for any application that requires accuracies higher than those typically demonstrated by industrial robotic arms. By conducting drilling trials with only corrections for the robot positional error applied, it will serve as a baseline for how

*Research conducted as part of the Made Smarter Connected Factories programme, funded by the Engineering and Physical Sciences Research Council (EPSRC).

[1]Although 'semi-automated' can cover a wide variety of assisted drilling methodologies, it typically relates to the use of a hand-held automated drilling unit that provides fixed cutting speed and feed, and so still requires significant manual input to position for each hole.

J. Moore, C. Burkinshaw and D. Sawyer are all with the University of Sheffield Advanced Manufacturing Research Centre's Integrated Manufacturing Group, Factory 2050, Europa Way, Sheffield, S9 1ZA, UK (phone: 0114 215 8200; e-mail: j.moore@amrc.co.uk, c.burkinshaw@amrc.co.uk, d.sawyer@amrc.co.uk).

significant the improvement can be without process error correction, as little could be found in the literature that presents such corrections being applied to physical robotic drilling trials.

When considering the robot positional error, there are typically two main methods employed to generate a model: kinematics-based and kinematics-free [9]. Kinematics-based models rely on developing an accurate kinematic model of the robot under test, whereas kinematics-free models treat the robot kinematics as a black-box, and instead rely on machine learning (ML) to determine the relationship between the input (i.e. programmed position) and the output (i.e. actual attained position or positional error). The former often requires an in-depth understanding of the construction of the robot arm, including all the potential error sources (e.g. stiffness, gear backlash, encoder accuracy, etc.) [10], all of which may be affected by the operational life of the robot. This means identical robot arms under different operating conditions could end up with different kinematic performances over time; so an understanding of how these errors propagate would also be required. It is for these reasons that generic kinematic models, even for a single model of robot arm, are difficult to develop. Although kinematics-free models are also subject to changes in performance over time or under differing conditions, it is generally a simpler task to re-capture the necessary data and retrain the model. This could be done at regular intervals, similar to calibration cycles, or when the accuracy of the robot drops below a certain level.

To try and develop a simple methodology that would be feasible to employ within an industrial setting, this paper focusses instead on the kinematics-free approach; training a ML model to improve the positional accuracy of an industrial robotic drilling platform. This approach has been demonstrated by McGarry et al. [11], who demonstrated that support vector regression model was able to reduce the maximum positioning error of a collaborative robot in x, y, and z from 2.239 mm, 6.107 mm and 3.636 mm, down to 0.252 mm, 0.595 mm and 0.896 mm, respectively. Similarly, Jiang et al. [12] utilised a back-propagation artificial neural network to reduce the maximum error in positioning of a collaborative robot from 3.993 mm to 0.656 mm.

The proposed methodology relies upon positional data to be captured from a laser tracker to initially train the model. However, unlike methods that require continuous online feedback from the measurement system such as those proposed by Stadelmann et al. [6] and Gharaaty et al. [7], this methodology allows the position of the robot to still be corrected once the measurement system has been removed.

This paper is organised as follows: Section II describes the platform upon which the testing took place, as well as the measurement equipment used; Section III outlines the method used for capturing data and the subsequent training and testing of the system; Sections IV and V present the results and discussion, respectively; and the conclusions and further work are provided in Section VI.

II. Equipment

The following sections provide details on the robotic drilling platform used (Section A), including information on the cutting tools and workpiece material used for the drilling trials; and the metrology equipment used for training and validation (Section B).

A. Robotic drilling platform

The platform used for this research (known as VIEWS) consisted of a KUKA KR240 R2900 Ultra with a drilling end effector, including pressure foot. The cell also includes a large reconfigurable fixturing solution, allowing workpieces to be mounted over a wide area of the working volume of the robot, which is shown in Figure 1. Despite this work focussing on correcting only robot positioning error, utilising the VIEWS platform allows data to be captured under conditions representative to robotic drilling (i.e. with the mass of a drilling end effector mounted); as well as during rphysical drilling trials through measuring hole positions. The drilling trials were conducted in coupons of aluminium 5083 using 10mm solid carbide drill bits.

B. Metrology and analysis equipment

The measurement of the robot's tool centre point (TCP) position was conducted using a Leica AT960 laser tracker in conjunction with a Leica T-Mac (Tracker-Machine control sensor) which allows measurements in six degrees of freedom. The T-Mac was mounted onto the drilling end effector and had previously been measured so that the relation between this and the TCP was known. A Leica T-Probe was also used in conjunction with the AT960 to measure the locations of holes once drilled.

Measurement data was captured by a PC running *SpatialAnalyzer* (SA) software, whilst a custom script in *MATLAB* was used to capture the 'reported' positional data (i.e. the TCP and individual joint position of the robot reported by the encoders) from the robot controller via an OPC UA server setup on the platform's PLC.

III. Method

This section explains the steps taken to develop the accuracy improvement algorithm, and how it was tested. There were two regimes under which this was done. The first being simple robot TCP positioning relative to the robot base frame (RBF); and the second being drilling trials relative to a common datum (CD). The reason behind testing these two

Figure 1: The robotic drilling cell with reconfigurable fixturing.

regimes was two-fold. The RBF scenario was a more straightforward test, relying on no other external frames to be setup and translated into. This allowed for any accuracy improvements to be gauged easily, and so the methodology could be trialled in a straightforward manner.

The introduction of a CD was opted for during the drilling trials, as it is common within industry for operations to be conducted relative to a datum that is either defined on a fixture or on a feature of the workpiece itself. This could therefore provide the evidence that accuracy improvements can be achieved under both regimes.

A. Corrections relative to the robot base frame

The RBF is the frame in which all robot's motions are conducted. It is therefore a requirement to measure it to be able to gauge the robot's accuracy as per ISO 9283:1998 [13]. As the RBF is typically located within the body of the robot, it is not possible to measure this directly, and so instead must be inferred experimentally.

1) Measurement of the robot base frame

There are several ways that the RBF measurement can be achieved. For this work, the RBF of the KUKA robot was measured using a laser tracker and employing the method described as the 'robot base frame general construction process' by McGarry et al. [14]. In summary, this involved best fitting a circle by measuring the robot whilst rotating joint 1; the centre of which when projected onto the plane of the robot's mounting plate gave the origin and z-direction (i.e. the normal to the circle). The frame alignment can then be fixed by best fitting a line measured during a motion of joint 2 when joint 1 is fixed at 0 degrees. To ensure backlash was accounted for, this second step was repeated with the movement of joint 1 to 0 degrees conducted from both a positive and negative direction, with the midpoint between the best fit lines taken as the final x-direction.

With the data from the measurement of the RBF loaded into the SA software, any subsequent measurements taken of the robot would provide the TCP in relation to the RBF.

2) Measuring the robot error

To gather the error in the robot's positional accuracy, a program was written to drive the robot in cartesian space to a grid of positions distributed across the working volume of the fixture (i.e. over the flexible fixturing solution). Although drilling in aerospace often involves operations in a range of orientations, to simplify the data capture and testing requirements at this stage, it was decided that the grid would be constructed in the plane of fixed z-height of 750 mm (just above the fixturing), and the drilling end effector would be fixed in a vertical orientation to emulate drilling a flat component laid horizontally across the fixture. This meant B and C of the robot had to be fixed at 0 deg and 180 deg, respectively; and A was fixed at 30 deg to ensure the T-Mac could be measured by the laser tracker at all points across the working volume.

The vertical orientation of the end effector put constraints on the reach of the robot, and so the grid was constructed to be between -1000 mm and +1000 mm in y, and 1400 mm and 2400 mm in x, with spacings of 100 mm in both directions. This resulted in a total of 232 points arranged as shown in Figure 2.

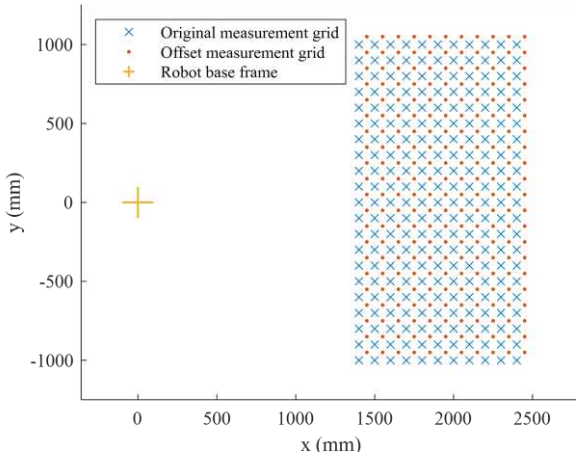

Figure 2: The measurement grids with respect to the robot base frame.

The robot was programmed to move the TCP to each of these x-y coordinates at 800 mm in z. At each location, it would lower the TCP to the desired 750 mm z-height, dwell for 5 seconds, then retract to 800 mm before moving to the next location as this emulates the motion conducted whilst undertaking drilling operations.

The tracker was configured in SA to measure the TCP when the T-Mac was detected as being stable, meaning a measurement was automatically captured at each of the dwell locations. The OPC UA MATLAB script was also run in parallel to capture the reported TCP values and joint positions.

The resulting OPC UA data and tracker data was then combined into a table comparing the 'desired' and 'attained' TCP positions, with each location represented by an individual row. It was then simple to add in two additional columns to the table consisting of the calculated error in x (x_{error}) and y (y_{error}) of the TCP, respectively:

$$x_{error} = x_{attained} - x_{desired} \quad (1)$$

$$y_{error} = y_{attained} - y_{desired} \quad (2)$$

where $x_{attained}$ and $y_{attained}$ are the measured position of the robot TCP, and $x_{desired}$ and $y_{desired}$ are the desired (nominal) TCP location.

3) Training the models

MATLAB's Regression Learner application was utilised on the resulting table to train models that could predict x_{error} and y_{error}, respectively. $x_{desired}$ and $y_{desired}$ were used as the inputs (predictors) to the models, with x_{error} or y_{error} being the output (response). It should be noted that as this application can only train models with single response variables, separate models for x_{error} and y_{error} had to be developed. Five-fold cross validation was used for the initial training/testing process, as well as 10% of the data being held back from to act as unseen data for final testing purposes. The Regression Learner application allowed 26 different types of regression model to be trained for each response, including models ranging from simple linear regression models to more complex neural networks. By identifying the model with the lowest validation and test root mean squared error (RMSE) values (presented in Figure 3), it was straightforward to select the most accurate model for predicting x_{error} and y_{error}, respectively.

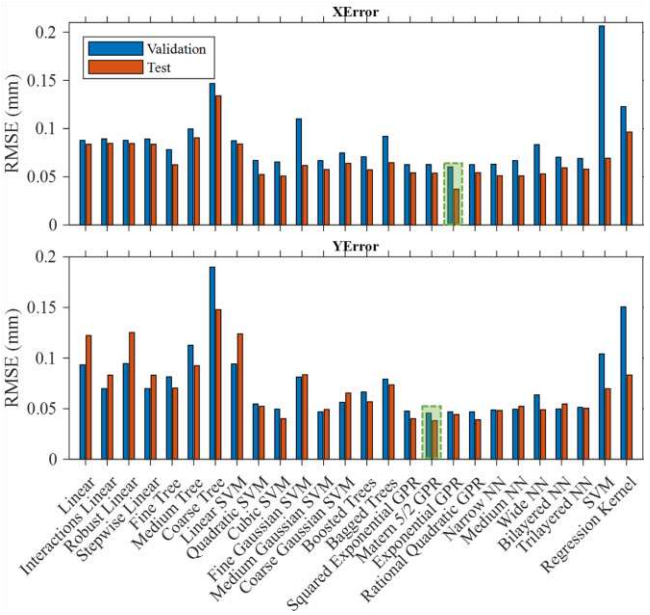

Figure 3: Comparison of the various model validation and test RMSE values when trained to predict x_{error} and y_{error}, respectively (selected models highlighted in green).

In this case Gaussian process regression (GPR) models with an exponential kernel and Matern 5/2 kernel were selected for having the lowest root mean squared errors (RMSEs) when predicting x_{error} and $y_{error,}$ respectively. Hyperparameter tuning was not investigated and so the default hyperparameters in the Regression Learner application were selected.

4) Testing and validation

The selected GPR models were used to update the programmed x and y positions ($x_{corrected}$ *and* $y_{corrected}$, respectively*)* for each point in the measurement grid using the following equations:

$$x_{corrected} = x_{desired} - x_{predicted\ error} \quad (3)$$

$$y_{corrected} = y_{desired} - y_{predicted\ error} \quad (4)$$

where $x_{predicted\ error}$ and $y_{predicted\ error}$ are the outputs from each of the x and y models, respectively.

To test the models' capabilities in interpolating and extrapolating, a second measurement grid was constructed (as shown in Figure 2). This was identical to the original nominal measurement grid in size, shape, and number points; but was offset by +50 mm in both x and y. This meant each point was situated in a location where the robot positioning error had not been measured previously, and so unseen by the models. These desired offset coordinates also went through the correction process provided by the GPR models to give $x_{corrected}$ *and* $y_{corrected}$ for the offset grid.

Once the robot program had been updated to include all of the corrected values (both from the original and offset grids), the same process as described in Section III.A.2) was repeated to measure the residual error of the robot TCP when revisiting these locations.

B. Corrections relative to the common datum

To ensure that this methodology is also effective in a situation where operations are relative to a frame defined by something external to the robot (e.g. a feature on the component, part of a fixture, etc.), the model was re-trained in a coordinate system defined by a CD.

1) Measurement of the common datum

In this case, the CD was defined as the centre of a SMR mounted at position **a** on the fixture when in drilling location 1, as shown in Figure 4. The orientation of the frame was set by measuring the SMRs **a**, **b** and **c** using the laser tracker which could then be used to define the y-z plane, and therefore the direction of x normal to this. The z axis direction could then be fixed by measuring the vertical direction between **d** and **e.**

By driving the robot close to the CD and measuring the robot's TCP using the T-Mac, it was possible to calculate the distance and rotation between the two frames in SA. The robot controller could then be updated with this information to define the CD as the robot's new working coordinate system.

2) Measuring the robot error

The robot TCP position was then remeasured whilst repeating a similar grid of positions to that of the original measurement grid. This used the same methodology as described in Section III.A.2), but this time with commanded positions and measurements relative to the CD rather than the RBF. From these measurements, a table containing x_{error} and y_{error} of the TCP relative to $x_{desired}$ and $y_{desired}$ in the CD frame could be calculated using Eq. (1) and (2).

3) Training the model

MATLAB's Regression Learner application was once again used to train and test two sets of models in predicting x_{error} and y_{error} with only $x_{desired}$ and $y_{desired}$ (relative to the CD) as predictors. It was found that the same GPR models (exponential and 5/2 Matern kernels) had the lowest RMSE values and so selected as the most effective in predicting x_{error} and y_{error} (for brevity, the results from these are omitted due to the similarity to those shown in Figure 3). This is perhaps unsurprising as the error map of the robot is unchanged – only a shift in the coordinate system. Corrections could again be provided for subsequent operations using (3) and (4).

4) Drilling trials

This time, rather than simply re-running the original or offset measurement grids, a set of drilling trials were conducted. As these were situated in arbitrary positions with respect to the CD, these would not fall perfectly on the previously measured positions, and so acted as an analogous test to the offset grid. These trials consisted of drilling a pattern of 6 holes (shown

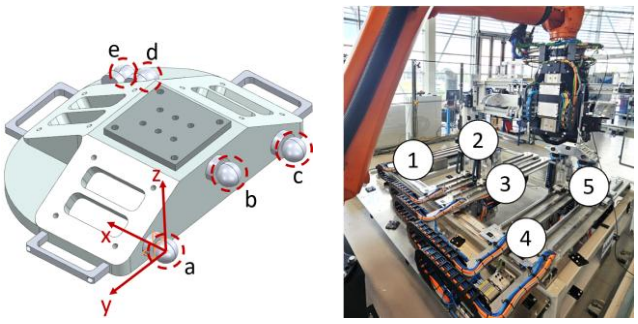

(a) (b)

Figure 4: Locations of (a) the common datum and SMRs (a-e) on the fixture; and (b) the fixture at different drilling locations (1-5) – with 1 being the location for the fixture when defining the common datum.

in Figure 5) in a coupon mounted to the top of the fixture when located at each of the 5 drilling locations (shown in Figure 4). This resulted in a total of 30 holes drilled across the platform's working volume. This was repeated both with and without corrections provided by the models to gauge the improvement in hole location.

The hole centre positions (HCPs) were determined by measuring 5 points around the internal circumference close to both the top and bottom surface of the coupon for each hole using the T-Probe. A best fit cylinder could then be constructed in SA for each hole, from which the HCP could be determined. It was then straightforward to gauge x_{error} and y_{error} in the drilled hole position using (1) and (2).

To help discriminate between robot positional error and the process error introduced by the drilling operation itself, the T-Mac was also measured whilst the robot was in position above each hole, immediately prior to the pressure foot being applied. This provided a measurement of the TCP with no process forces acting upon it – meaning the portion of the hole position error related solely to robot positional error could be determined for each hole.

IV. Results

A. Corrections relative to the robot base frame

The distribution of TCP errors for x and y relative to the RBF both before and after correction are illustrated in Figure 6. This includes the corrected measurements for both the original grid, and the offset grid. These results are quantified in Table I.

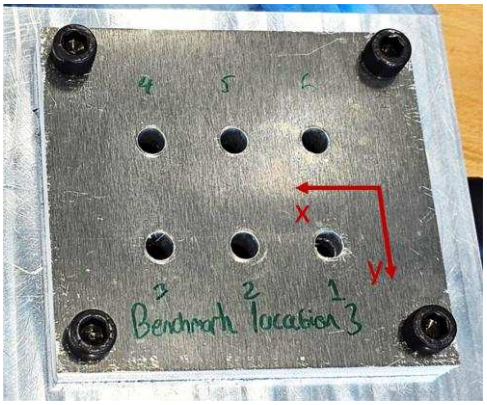

Figure 5: Example of the 6 holes drilled at each location – relative orientation of x and y axes provided for reference.

TABLE I. Tool Centre Point Error Reduction Relative to the Robot Base Frame for Both Original and Offset Grids

	Max error (mm)		Mean error (mm)	
	x	***y***	***x***	***y***
Uncorrected original	1.412	0.502	0.993	0.209
Corrected original	0.093	0.189	0.022	0.055
Corrected offset	0.235	0.174	0.085	0.051
Reduction original (%)	**93.4**	**62.4**	**97.7**	**73.5**
Reduction offset (%)	**83.4**	**65.3**	**91.4**	**75.8**

B. Corrections relative to the common datum

The distribution for HCP errors for x and y relative to the CD is shown in Figure . It should be noted that in this case, the error in y after correction increases. This is quantified in Table II. To help discriminate between robot positional error and process error, Figure shows the distribution of TCP errors for x and y relative to the CD immediately prior to the drilling operation. This is quantified in Table III.

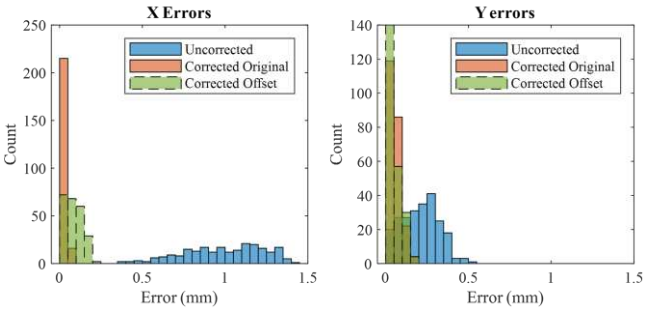

Figure 6: Comparison of the tool centre point errors (magnitude) in x and y measured relative to the robot base frame before and after correction for both the original and offset grids.

TABLE II. Hole Position Error Reduction Relative to the Common Datum

	Max error (mm)		Mean error (mm)	
	x	***y***	***x***	***y***
Uncorrected	0.945	0.598	0.688	0.261
Corrected	0.523	0.695	0.323	0.378
Reduction (%)[a]	**44.6**	**-16.3**	**53.0**	**-45.1**

a. where a negative number indicates an increase in error.

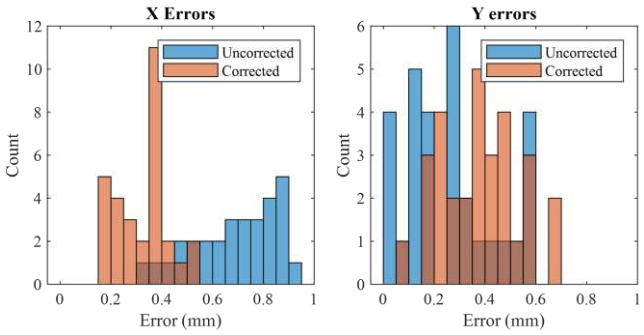

Figure 7: Comparison of the hole position errors (magnitude) in x and y measured relative to the common datum before and after correction.

TABLE III. Tool Centre Point Error Reduction Relative to the Common Datum Immediately Prior to Drilling

	Max error (mm)		Mean error (mm)	
	x	***y***	***x***	***y***
Uncorrected	0.503	0.421	0.180	0.164
Corrected	0.199	0.208	0.092	0.082
Reduction (%)	**60.5**	**50.7**	**48.8**	**50.3**

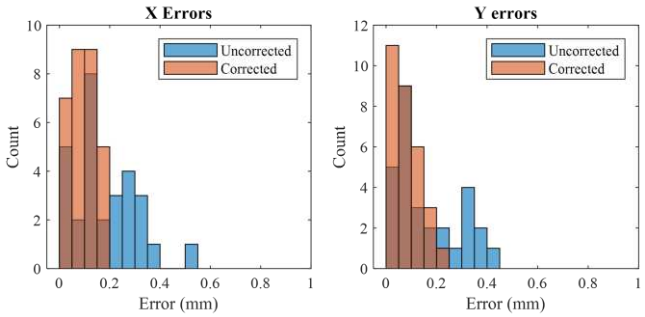

Figure 8: Comparison of the tool centre point errors (magnitude) in x and y measured relative to the common datum immediately prior to drilling; before and after correction.

V. Discussion

As can be seen in the distributions for TCP errors relative to the RBF (Figure 6), there is a significant reduction in the positional error for both the original and offset grids; with the maximum and mean errors being reduced by over 80% and 60% for x and y, respectively. There is a marginal reduction in the performance of the model in correcting errors in x for the offset grid compared with the original grid, but this is to be expected since the model is having to interpolate between trained positions. In fact, by examining the mean error values achieved for both original grid (0.022 mm in x, 0.055 mm in y) and offset grids (0.085 mm in x, and 0.051 mm in y), it can be seen that this open-loop methodology performs marginally better in correcting for static robot positioning error than the closed-loop models reported in the literature [6],[7] (between 0.050 mm and 0.10 mm).

The maximum error values for the original grid (0.093 mm in x, 0.189 mm in y) and offset grid (0.235 mm in x, and 0.174 mm in y) are also lower than the maximum error values achieved by McGarry et al. [11] (0.252 mm in x, 0.595 mm in y); and by Jiang et al. [12] (0.656 mm). This therefore demonstrates that the presented models are successful in achieving significant improvement of the positioning accuracy of the drilling platform across its working volume, including positions previously unseen by the models.

By interrogating the values presented in Tables I and III, it is possible to compare the performance of the models in correcting TCP error for the RBF and CD scenarios. Although the percentage reductions are lower for the CD scenario, it should be noted that the uncorrected maximum and mean errors are not as high as those in the RBF scenario. This could be due to the fact that the methodology used for measuring the CD provided a more accurate fit than that used to measuring the RBF. The CD could be measured directly using the T-Probe, whereas the RBF is inferred by measuring robot motion (as outlined in Sections III.B.1) and III.A.1), respectively). Therefore, by comparing the corrected maximum and mean errors, the values of the CD scenario are comparable to those of the corrected offset grid in the RBF scenario. This is to be expected as the positions used for the CD scenario were unseen by the model, analogous to the offset grid in the RBF scenario.

However, upon reviewing the distributions for hole position errors (Figure), the effectiveness of employing the models in physical drilling operations are not so clear.

Although there is a reduction in both maximum and mean hole position errors in x (44.6% and 53.0%, respectively); there is an overall increase in hole position error for y.

It is therefore thought that the majority of the hole position error is introduced by the drilling process. This is supported by the error values provided for the TCP immediately prior to drilling at each hole location. The maximum and mean errors for both x and y are reduced by around 50% or more, demonstrating that the model is still effective in these particular locations.

It is hypothesised that the increase in hole position error in the y direction after correction could be due to the drilling process introducing error in the same direction as the correction provided by the model. This means that in the uncorrected case, the drilling error moves the hole position closer to the desired position. However, when the correction from the model is applied, the combination of the drilling process error and the correction makes the final hole position overshoot the desired position, thus increasing the error.

This means that although the models are successful in correcting for the robot positional error, this may not always be suitable when attempting to improve the accuracy of an overall process being undertaken by a robotic platform. A model that also takes into account of the process errors may be more successful.

VI. Conclusions and Further Work

This paper has demonstrated the effectiveness of an open-loop methodology based on GPR models in reducing robot positional errors. This methodology was able to reduce the mean positioning error of a robotic drilling platform by 97.7% and 73.5% in x and y, respectively; with mean error values achieving comparable values to those achieved by closed-loop methodologies in the literature.

However, it has also highlighted the potential downsides of using such open-loop methodologies in real-world applications. When utilising the same methodology during drilling operations, the reduction in mean hole position error in x was significantly lower (only 53.0%), and the maximum error in y *increased* by 45.1%. This was thought to be due to the model providing corrections in the same direction as the error introduced by the drilling process causing the final hole position to overshoot the desired location.

Despite these complications, the overall methodology of open-loop correction for improving robot accuracy has been demonstrated successful. This can be useful in many applications where process forces are less of an issue (eg. inspection, welding, additive manufacturing, etc.).

Further work is still required to address the main drawback of this open-loop methodology; namely the introduction of process forces. Although it might be possible to develop a single model to account for both robot positional errors and process errors, it might be advantageous to develop a modular methodology.

This modular methodology could be made up of an initial model that corrects for robot positional error, and a process

error model then augments the correction based on the process being undertaken. This could then allow the process error model to be swapped or updated based on the particular process being undertaken without the need for a comprehensive re-measurement of the robot across the entire volume. This could be particularly advantageous where a robotic platform equipped with a tool changer can utilise a number of end effectors to undertake a range of different operations.

The methodology presented was also limited to testing on a two-dimensional plane – focussing on the drilling of flat components. In real-world applications, there is a need for drilling operations to be undertaken at various heights and orientations (particularly for aerospace). It would therefore be beneficial to develop models that can work across the entire configuration space (rather than task space) of the robotic platform.

Other work could include development of a model that can improve the accuracy of milling operations. This is particularly challenging due to the more dynamic nature of milling compared with drilling. This would therefore require continuous updates to be provided to the robot controller based on its live location and machining parameters, rather than discrete corrections based on each hole location.

ACKNOWLEDGMENT

The authors would like to thank EPSRC in supporting this research as part of the Made Smarter Connected Factories Programme. For the purpose of open access, the authors have applied a Creative Commons Attribution (CC BY) licence to any Author Accepted Manuscript version arising from this submission.

REFERENCES

[1] Atlas Copco UK Holdings Ltd., 'The role of the manual drill in the aerospace manufacturing industry'. Accessed: Nov. 28, 2024. [Online]. Available: https://www.atlascopco.com/en-uk/itba/expert-hub/articles/the-role-of-the-manual-drill-in-the-aerospace-manufacturing-industry

[2] Applied Fasteners and Tooling, 'Understanding the Different Types of Aerospace Drills'. Accessed: Mar. 07, 2025. [Online]. Available: https://aft.systems/understanding-the-different-types-of-aerospace-drills/

[3] BSI, 'BS EN 3201-2008 Aerospace series — Holes for metric threaded fasteners', May 2008.

[4] D. Chen, P. Lv, L. Xue, H. Xing, L. Lu, and D. Kong, 'Positional error compensation for aviation drilling robot based on Bayesian linear regression', *Eng Appl Artif Intell*, vol. 127, p. 107263, Jan. 2024, doi: 10.1016/J.ENGAPPAI.2023.107263.

[5] J. R. Diaz Posada, U. Schneider, S. Pidan, M. Geravand, P. Stelzer, and A. Verl, 'High accurate robotic drilling with external sensor and compliance model-based compensation', *Proc IEEE Int Conf Robot Autom*, vol. 2016-June, pp. 3901–3907, Jun. 2016, doi: 10.1109/ICRA.2016.7487579.

[6] L. Stadelmann, T. Sandy, A. Thoma, and J. Buchli, 'End-Effector Pose Correction for Versatile Large-Scale Multi-Robotic Systems', *IEEE Robot Autom Lett*, vol. 4, no. 2, pp. 546–553, Apr. 2019, doi: 10.1109/LRA.2019.2891499.

[7] S. Gharaaty, T. Shu, W. F. Xie, A. Joubair, and I. A. Bonev, 'Accuracy enhancement of industrial robots by on-line pose correction', *2017 2nd Asia-Pacific Conference on Intelligent Robot Systems, ACIRS 2017*, pp. 214–220, Jul. 2017, doi: 10.1109/ACIRS.2017.7986096.

[8] Y. H. Cho, D. Sawyer, C. Burkinshaw, and C. Scraggs, 'Robotic Drilling: A Review of Present Challenges', in *SAE Technical Papers*, SAE International, Mar. 2024. doi: 10.4271/2024-01-1921.

[9] D. Chen, P. Lv, L. Xue, H. Xing, L. Lu, and D. Kong, 'Positional error compensation for aviation drilling robot based on Bayesian linear regression', *Eng Appl Artif Intell*, vol. 127, p. 107263, Jan. 2024, doi: 10.1016/J.ENGAPPAI.2023.107263.

[10] H. N. Nguyen, J. Zhou, and H. J. Kang, 'A calibration method for enhancing robot accuracy through integration of an extended Kalman filter algorithm and an artificial neural network', *Neurocomputing*, vol. 151, no. P3, pp. 996–1005, Mar. 2015, doi: 10.1016/J.NEUCOM.2014.03.085.

[11] L. McGarry *et al.*, 'Machine Learning Methods to Improve the Accuracy of Industrial Robots', in *SAE International Journal of Advances and Current Practices in Mobility*, SAE International, Mar. 2023, pp. 1900–1918. doi: 10.4271/2023-01-1000.

[12] Y. Jiang, L. Yu, H. Jia, H. Zhao, and H. Xia, 'Absolute Positioning Accuracy Improvement in an Industrial Robot', *Sensors 2020, Vol. 20, Page 4354*, vol. 20, no. 16, p. 4354, Aug. 2020, doi: 10.3390/S20164354.

[13] British Standards Institution, 'BS EN ISO 9283:1998 - Manipulating industrial robots - Performance criteria and related test methods', 1998.

[14] L. McGarry, J. Butterfield, and A. Murphy, 'Assessment of ISO Standardisation to Identify an Industrial Robot's Base Frame', *Robot Comput Integr Manuf*, vol. 74, p. 102275, Apr. 2022, doi: 10.1016/J.RCIM.2021.102275.